Published in final edited form as:
Growth Factors. 2008 August ; 26(4): 226–237. doi:10.1080/08977190802277880.

BMP-2 vs. BMP-4 expression and activity in glucocorticoid-arrested MC3T3-E1 osteoblasts: Smad signaling, not alkaline phosphatase activity, predicts rescue of mineralization

CYNTHIA A. LUPPEN[1,†], **RONALD L. CHANDLER**[2,3], **TOMMY NOH**[1], **DOUGLAS P. MORTLOCK**[2,3], and **BARUCH FRENKEL**[1,4]

[1]Department of Biochemistry and Molecular Biology, Keck School of Medicine, University of Southern California, Institute for Genetic Medicine, Los Angeles, CA, USA [2]Department of Molecular Physiology and Biophysics, Vanderbilt University School of Medicine, Nashville, TN, USA [3]Center for Human Genetics Research, Vanderbilt University School of Medicine, Nashville, TN, USA and [4]Department of Orthopaedic Surgery, Institute for Genetic Medicine, Keck School of Medicine, University of Southern California, Los Angeles, CA, USA

Abstract

Pharmacological glucocorticoids (GCs) inhibit bone formation, leading to osteoporosis. GCs inhibit bone morphogenetic protein-2 (*Bmp2*) expression, and rhBMP-2 restores mineralization in GC-arrested osteoblast cultures. To better understand how GCs regulate BMPs, we investigated *Bmp* transcription, as well as rhBMP-induced Smad and alkaline phosphatase (ALP) activity. *Bmp2* cis-regulatory regions were analyzed by reporter plasmids and LacZ-containing bacterial artificial chromosomes. We found that GCs inhibited *Bmp2* via a domain >50 kb downstream of the coding sequence. *Bmp* expression was evaluated by RT-PCR; whereas GCs strongly inhibited *Bmp2*, *Bmp4* was abundantly expressed and resistant to GCs. Both rhBMP-2 and rhBMP-4 restored mineralization in GC-arrested cultures; rhBMP-2 was 5-fold more effective when dosing was based on ALP activation, however, the rhBMPs were equipotent when dosing was based on Smad transactivation. In conclusion, GCs regulate *Bmp2* via a far-downstream domain, and activation of Smad, not ALP, best predicts the pro-mineralization potential of rhBMPs.

Keywords

Osteoblast; BMP; Smad; alkaline phosphatase; glucocorticoids

Introduction

Chronic glucocorticoid (GC) treatment induces bone loss and increases fracture risk (Van Staa et al. 2000; Mazziotti et al. 2006). Unlike post-menopausal osteoporosis, which is associated with increased bone resorption and high bone turnover, glucocorticoid-induced osteoporosis (GIO) is characterized by low bone turnover (Godschalk and Downs 1988; Prummel et al. 1991; Dempster et al. 1997; Pearce et al. 1998). Although, systemic

Correspondence: B. Frenkel, Keck School of Medicine, University of Southern California, Institute for Genetic Medicine, 2250 Alcazar Street, CSC/IGM240, Los Angeles, CA 90033, USA. Tel: 1 323 442 1322. Fax: 1 323 442 2764. frenkel@usc.edu.
[†]Current address: Stanford University School of Medicine, Institute for Stem Cell Biology, Palo Alto, CA, USA.

Declaration of interest: The authors report no conflicts of interest. The authors alone are responsible for the content and writing of the paper.

mechanisms of disease were initially proposed, including hypocalcemia and hypogonadism, GIO is mostly attributed to direct deleterious effects of GCs on cells in the osteoblast lineage, in particular inhibition of proliferation and stimulation of apoptosis (Weinstein et al. 1998; Canalis and Delany 2002; Liu et al. 2004; O'Brien et al. 2004; Mazziotti et al. 2006). Independent of the resulting decrease in bone formation and bone mass, GCs also decrease bone strength, possibly due to osteocyte apoptosis (O'Brien et al. 2004).

Under permissive conditions, cultured pre-osteoblasts proliferate, condense and form nodules, where a collagenous extracellular matrix is elaborated and eventually mineralizes (Owen et al. 1990). In the non-transformed MC3T3-E1 cell line (Sudo et al. 1983; Wang et al. 1999), as well as in primary murine osteoblast cultures (Noh and Frenkel, unpublished observations 2006), administration of 0.1–1 μM dexamethasone (DEX) at a defined developmental stage strongly inhibits cell cycle progression and mineral deposition (Smith et al. 1999). Since GCs do not induce apoptosis in differentiating MC3T3-E1 cultures (Zalavras et al. 2003), the effects of GCs on osteoblast growth and differentiation can be studied apart from apoptosis. The bone morphogenetic protein-2 (*Bmp2*) gene, whose human orthologue regulates bone mass (Styrkarsdottir et al. 2003), is strongly suppressed in DEX-treated MC3T3-E1 cultures (Luppen et al. 2003b), and co-treatment with rhBMP-2, even for a brief 6-h period, restores osteoblast differentiation and mineral deposition (Luppen et al. 2003a).

BMPs are secreted proteins that belong to the TGF-β superfamily, and have diverse effects on cell proliferation, differentiation and function. Threshold doses of particular BMPs play developmental roles (Liu et al. 2005) that are tightly regulated by diverse ligands, receptors and inhibitors, as well as inputs from other signaling pathways. BMP receptor complexes are multimeric configurations of type I and type II serine/threonine kinase receptors (Feng and Derynck 2005). The dynamics of ligand dimerization (Zhu et al. 2006), protein–receptor interactions (Greenwald et al. 2004; Harrison et al. 2004), and receptor assembly (Nohe et al. 2002) contribute to the specificity of BMP signaling (Feng and Derynck 2005). Activated type I BMP receptors interact with the BMP–Smads (Smads 1, 5, 8), mitogen activated protein kinases (MAPK) (Yu et al. 2002) and TGF-β activated kinases (Qiao et al. 2005). BMP signaling is therefore composed of Smad-dependent and -independent components (Derynck and Zhang 2003). There is increasing evidence that the Smad and MAPK pathways regulate different, essential aspects of osteoblast function (Lai and Cheng 2002; Nohe et al. 2002; Guicheux et al. 2003; Hu et al. 2003).

BMPs were originally named for their ability to induce ectopic bone formation (Urist 1965). More than 20 BMPs have since been identified and most of them, including the "osteogenic" BMPs (BMPs 2, 4–7, and 9), have been assigned roles in a variety of developmental processes. In this paper, we focus on BMP-2 and BMP-4, which are highly homologous proteins [86% identity of the mature human peptides (Celeste et al. 1990)] that act during organogenesis, bone formation and bone repair. Divergent developmental roles for BMP-2 and BMP-4 have been described: the expression of BMP-4, but not BMP-2 or BMP-7, correlated with upper beak morphology in birds (Abzhanov et al. 2004; Wu et al. 2004); the expression of BMP-2, but not BMP-4 or BMP-7, was shown to be responsible for the extra-long digits that facilitate wing formation in bats (Sears et al. 2006). Recently, retrovirally produced BMP-2 and BMP-4 have been shown to synergize differently with vascular endothelial growth factor during muscle-derived stem cell therapy for bone healing (Peng et al. 2005). Are BMP-2 and BMP-4 regulated differentially during osteoblast differentiation and/or in response to GCs? Although, a few *in vitro* studies have described the efficacy of one recombinant BMP over another (Boden et al. 1996; Cheng et al. 2003), the expression and signaling of endogenous BMPs have not been compared in osteoblasts. Furthermore, the regulation of BMPs in bone is increasingly important as genetic polymorphisms in *BMP2*

have been correlated with familial osteoporosis (Styrkarsdottir et al. 2003). In this paper, we compare Bmp-2 and Bmp-4 from two related aspects: regulation by GCs and ability to restore mineralization in GC-arrested MC3T3-E1 cultures.

Materials and methods

Reagents

To maintain the MC3T3-E1 cell line, α-minimum essential medium and penicillin/streptomycin were obtained from Invitrogen Corp. (Carlsbad, CA, USA). Individual lots of fetal bovine serum, also from Invitrogen, were selected based on their ability to support mineralization. Ascorbic acid, β-glycerophosphate and DEX were purchased from Sigma (St Louis, MO, USA). rhBMP-2 that was produced in CHO cells was generously provided by Wyeth Research (Cambridge, MA, USA), and rhBMP-4 that was produced in NSO mouse myeloma cells was purchased from R&D Systems (Minneapolis, MN, USA). SDS-PAGE and Coomassie blue staining of the two rhBMPs was used to assess purity and confirm their relative label concentrations. Cell culture dishes were purchased from Corning Incorporated (Corning, NY, USA). Reagents for the biochemical measurement of alkaline phosphatase (ALP) and DNA were obtained from Sigma. The *o*-nitrophenyl β-D-galacto-pyranoside (ONPG) substrate for the β-galactosidase assay was purchased from Pierce Biochemical (Rockford, IL, USA). Protein content was measured using the MicroBCA assay kit (Pierce Biochemical). The histological assays utilized Alizarin Red (Sigma) and the β-gal staining kit (Invitrogen). RNA isolation was accomplished using the Aurum™Total RNA Mini Kit (Bio-Rad, Hercules, CA, USA). The Ambion DNA-free™ kit (Austin, TX, USA) was used to remove DNA prior to reverse transcription with the Thermoscript RT-PCR system (Invitrogen). Transfection of plasmid constructs was carried out using the Lipofectamine 2000 reagent (Invitrogen). Luciferase constructs based on the mouse *Bmp2* promoter, and the BMP-specific Smad-binding element reporter $(GCCG)_{12}$-luciferase, were generously provided by Drs. Ming Zhao and Stephen Harris (University of Texas Health Sciences Center, San Antonio, TX, USA). The Luciferase Assay System was purchased from Promega Corporation (Madison, WI, USA).

Cell culture

A robustly mineralizing subclone of the MC3T3-E1 cell line (Smith et al. 1999) was used in this study. Cells were plated at a density of 30,000/cm^2 in 6- or 12-well plates for RNA isolation, histological, biochemical and reporter assays, and in 100 mm plates to harvest sufficient cells for electroporation. Cells were maintained in α-minimum essential medium supplemented with 10% fetal bovine serum and 1.5% penicillin/streptomycin. Starting at 80% confluency (typically, day 3, after plating on day 0), the culture medium was supplemented with 50 μg/ml ascorbic acid and 10 mM β-glycerophosphate to support differentiation.

Histological assays

For Alizarin Red staining of calcium, culture wells were washed once in phosphate-buffered saline (PBS) and fixed for 1 h at 4°C in 70% ethyl alcohol. The Alizarin Red solution (40 mM, pH 4.2) was filtered through Whatman paper, then applied to the fixed wells for 10 min at room temperature. Non-specific staining was removed by several washes in water. β-gal staining was performed according to manufacturer's protocol. Briefly, cultures were washed with PBS, then fixed for 10 min at room temperature with a formaldehyde-containing solution. After the fixative was removed, a solution containing the X-gal substrate was added. The colorimetric X-gal reaction was allowed to proceed during a 2 h incubation at 37°C. Histological outcomes were evaluated by brightfield microscopy.

Biochemical assays

Cell extracts for ALP, protein and DNA assays were collected by scraping in a 10 mM Tris–Saline buffer (pH 7.2) containing 0.2% Triton X-100. ALP activity was measured using the *p*-nitrophenyl phosphate substrate, and protein content was determined using the MicroBCA kit. To measure DNA, aliquots of the cell extracts were acid-hydrolyzed (final concentration 0.5 N HCl), and then reacted with diaminobenzoic acid (Luppen et al. 2003b). The spectrophotometric analyses of protein (562 nm) and ALP (410 nm) were conducted using a Power WaveX microplate scanning spectrophotometer (Biotek Instruments, Winooski, VT, USA). The fluorometric analysis of DNA content (excitation 400 ± 15 nm, emission 485 ± 10 nm) was performed on a Perkin-Elmer VICTOR (Perkin-Elmer Life Sciences, Inc., Boston, MA, USA). For the β-gal biochemical assay, cell extracts were collected in reporter lysis buffer and then reacted with ONPG substrate. β-gal activity (420 nm) was assessed by spectrophotometric analysis, as described above.

PCR and RT-PCR

Genomic DNA was isolated with a standard buffer containing 0.5% SDS, RNase and Tris–EDTA (pH 8) followed by phenol/chloroform extraction. RNA was isolated and treated with DNase prior to reverse transcription. Reverse transcription was carried out on 2 μg of denatured RNA using the Thermoscript RT-PCR system according to the manufacturer's protocol. First strand cDNA synthesis was primed with poly dT primers. The cDNAs were PCR amplified (MJ Research, Inc., Waltham, MA, USA) in a total volume of 25 μl. The reaction included 1 μCi (800 Ci/mmol) of deoxycytidine 5′-[α-32P] triphosphate (Perkin-Elmer Life Sciences). For each of the genes analyzed, a standardcurve was performed in paralleltoensureclose-to-linear amplification conditions. The amplified PCR products were resolved by electrophoresis on a 5% polyacrylamide gel. The polyacrylamide gels were dried and exposed to a storage phosphor screen (Molecular Dynamics, Sunnyvale, CA, USA) and the signal associated with the PCR products was detected using the STORM 840 Phosphor Analyzer and Image Quant software (Molecular Dynamics). The five sets of primers used in this paper are listed in Table I.

Transfections and reporter assays

Transient transfection was performed using the Lipofectamine 2000 reagent according to the manufacturer's protocol. Briefly, cultures were transfected at 90% confluency, and the lipid-DNA complexes were removed following 4–6 h of incubation at 37°C. After the specified experimental treatment, cell layers were lysed and stored at −80°C until processing. Subsequently, lysates were thawed and reacted with the luciferin substrate supplied in the Promega Luciferase System. Luciferase activity was analyzed using a Perkin-Elmer VICTOR luminometer (Perkin-Elmer Life Sciences), and corrected for protein content. The BMP–Smad reporter, $(GCCG)_{12}$-luciferase, was stably transfected (Lipofectamine) into cultures by cotransfection with the pCEP4 plasmid (Invitrogen), containing a hygromycin resistance gene, at a 15:1 molar excess. Colonies were selected and expanded under continuous treatment with 100 μg/ml hygromycin. Lysates from the $(GCCG)_{12}$-luciferase stably transfected cultures were collected and assayed as described above.

Construction of two *Bmp2* BAC reporters used in this study was described previously (Chandler et al. 2007). These reporters were derived from mouse clones RP23-85011 ("5′ BAC") and RP23-409L24 ("3′ BAC"), which were identified using the UCSC genome browser (Kent et al. 2002) and obtained from the Children's Hospital Oakland Research Institute. Each reporter BAC contains an IRES-β-geo cassette in place of *Bmp2* exon 3 mature region coding sequences. The *Bmp2*-LacZ BAC reporter constructs were stably transfected into MC3T3-E1 cultures by electroporation. Approximately 1.5×10^6 MC3T3-E1 cells were typsinized, washed with PBS, and reconstituted in 400 μl serum-free Opti-

MEM containing 1.25% DMSO (Melkonyan et al. 1996). The cells were transferred into pre-chilled 0.4 cm Gene Pulser cuvettes (Bio-Rad) and kept on ice. Using wide bore pipette tips, 20 μg of BAC DNA was gently introduced into each cuvette. The cuvettes containing the cells and BAC DNA were incubated at room temperature, with occasional agitation, for 1 min, and then subjected to an electric current. The electric current was generated using a Bio-Rad Gene Pulser II apparatus with the following settings: 0.25 kV voltage, 0.55 kV/cm field strength, 960 μF capacitance. Time constants of approximately 60 ms were obtained. Following electroporation, the cuvettes were incubated on ice for 2–10 min, then the contents of each cuvette were transferred into individual wells of a 6-well plate containing α-minimum essential medium with 1.25% DMSO. The plated cells were allowed to recover for 24 h before serum-containing medium was added. After 24 h, the medium was replaced with α-minimum essential medium with 10% serum, 1.5% penicillin/streptomycin, and 1.25% DMSO. In addition, 100 μg/ml neomycin was added with the first medium change, and all subsequent changes, to select for stably transfected cells. Stable cell pools were expanded from 5 to 10 colonies each. *Bmp2*-LacZ expression was detected using the β-gal histological and biochemical assays described above.

Statistical analysis

When appropriate, means ± standard deviations were compared using the Student's *t*-test. Differences were considered significant, when $p \leq 0.05$. Statistical analyses were conducted using GraphPad InStat version 3.0a for Macintosh (GraphPad, San Diego, CA, USA).

Results

DEX inhibits Bmp2, but not Bmp4 expression or BMP–Smad activity, in MC3T3-E1 cultures

We initially investigated whether the inhibitory effects of GCs on the osteoblast phenotype and on *Bmp2* gene expression (Luppen et al. 2003b) were associated with inhibition of the closely related *Bmp4* gene. We reverse transcribed and amplified *Bmp2* and *Bmp4* mRNA from day-5 MC3T3-E1 osteoblast cultures that had been maintained under differentiation conditions with or without 1 μM DEX for 48 h. Using primers that anneal to exons 1 and 3 of *Bmp2* and to exons 2 and 3 of *Bmp4* (Figure 1A, black arrows), we were able to detect both *Bmp2* and *Bmp4* mRNA in CONTROL cultures (Figure 1(B)). As previously reported (Luppen et al. 2003b), DEX strongly inhibited *Bmp2* expression; however, *Bmp4* expression was not changed (Figure 1(B)). Equivalent RNA input and reverse transcription were verified by amplification of the ribosomal protein L10A mRNA, whose expression is not altered by DEX treatment (Leclerc et al. 2004).

If there were no fundamental differences in the translation, secretion or activity of BMP-2 vs. BMP-4, then the strong inhibition of *Bmp2* would be meaningful, only if its basal expression was significantly higher than that of *Bmp4*. To determine the relative abundance of these mRNAs in our cultures, we performed an additional RT-PCR assay using single-exon primers for *Bmp2* (exon 3) and *Bmp4* (exon 3) (Figure 1(A)). This allowed us to use genomic DNA as template and to demonstrate that the respective sequences were amplified with comparable efficiency (Figure 1(C), *left*). Under these conditions, *Bmp2* mRNA could not be detected even with cDNA input 16-fold higher than the input at which *Bmp4* mRNA was readily detectable (Figure 1(C), *right*). We were able to detect *Bmp2* mRNA, only when we further increased the cDNA input by an additional 5-fold (as seen in Figure 1(B), top row, CONTROL lane).

If, as suggested by Figure 1(C), *Bmp4* expression far exceeds that of *Bmp2*, then the DEX-mediated repression of *Bmp2* may have few, if any, functional consequences under these conditions. To test this interpretation, we assessed the effect of DEX on BMP–Smad

signaling. We employed the $(GCCG)_{12}$-luciferase reporter construct (Zhao et al. 2002), which contains 12 repeats of GCCGCCGC, a Smad-binding motif first identified in the enhancer regions of many Drosophila genes, such as *tinman, vestigial, labial* and *ultrabithorax*. This motif also binds mammalian BMP-specific, but not TGF-β-specific Smads (Kusanagi et al. 2000). Cultures stably transfected with the $(GCCG)_{12}$-luciferase reporter were treated with DEX for 48 h. As shown in Figure 1(D), luciferase activity in the DEX-treated cultures was equivalent to that in CONTROL cultures, suggesting that DEX inhibition of *Bmp2* does not significantly impact overall BMP signaling. Thus, DEX dramatically inhibited *Bmp2* expression, but did not have the same strong effect on *Bmp4* or overall BMP activity. We also noted that rhBMP-2 stimulated BMP–Smads far beyond the levels measured in untreated cultures (Figure 1(D)).

While assessing the effect of DEX on BMP–Smad signaling, we included as a positive control treatment of the $(GCCG)_{12}$-luciferase cells with rhBMP-2. As expected, this treatment resulted in robust stimulation of luciferase activity, validating responsiveness of the reporter to BMP signaling (Figure 1(D)). It is noteworthy, however, that the specific treatment—with 100 ng/ml rhBMP2 for 48 h—resulted in supra-physiological BMP signaling, 8- and 12-fold stronger than the levels measured in CONTROL and DEX-treated cultures, respectively (Figure 1(D)).

rhBMP-2 and -4 similarly stimulate ALP activity, yet rhBMP-4 does not match the anti-GC pro-mineralization activity of rhBMP-2

The DEX-mediated repression of *Bmp2* mRNA could have a significant functional outcome, if BMP-2 was more potent than BMP-4. We obtained recombinant preparations of rhBMP-2 and rhBMP-4 and confirmed their purity by Coomassie staining of a protein gel (data not shown). Since ALP activity is commonly used to infer BMP responsiveness, we measured ALP activity 24 h after administration of either rhBMP-2 or rhBMP-4 to DEX-treated cultures. As shown in Figure 2(A), the two BMPs stimulated ALP activity in a dose-dependent manner with comparable potency over a concentration range of 0–100 ng/ml (Figure 2(A)).

We have previously shown that brief exposure to rhBMP-2 is sufficient to restore deposition of apatite-like mineral in GC-inhibited MC3T3-E1 cultures (Luppen et al. 2003a). If ALP activation were responsible for this rescue, then rhBMP-4 would have been able to rescue mineralization in GC-inhibited MC3T3-E1 cultures with comparable efficiency. We initially compared the induction of mineral deposition by the two BMPs at 100 ng/ml. As shown in the schematic of Figure 2(B), MC3T3-E1 cultures were treated with DEX from day 3, and then briefly exposed (10 h) to either rhBMP-2 or rhBMP-4 on day 5. DEX administration was continued until day 14, at which time calcium deposition was evaluated by Alizarin Red staining (Figure 2(B)). As previously reported, DEX treatment strongly inhibited mineral deposition relative to CONTROL cultures and brief rhBMP-2 exposure restored mineral deposition in DEX cultures to CONTROL levels (Luppen et al. 2003a). Surprisingly, however, rhBMP-4, which had stimulated ALP activity to the same extent as rhBMP-2 (Figure 2(A)), did not rescue DEX-inhibited calcium deposition (Figure 2(B)).

Differential rhBMP-2 and -4 stimulation of BMP–Smad activity parallels mineralization

The failure of rhBMP-4 to match rhBMP-2's anti-GC action with regard to mineralization is intriguing because the mature BMP-2 and BMP-4 proteins differ by only 16 out of 114 amino acids (Celeste et al. 1990) and because the two recombinant proteins equally stimulated ALP activity (Figure 2(A)). To address the enhanced mineralization potential of rhBMP-2 compared to rhBMP-4, we hypothesized that rhBMP-2 more potently stimulated BMP–Smads.

The Smad activation in response to rhBMP-2 and rhBMP-4 was assessed using MC3T3-E1 cells stably transfected with the $(GCCG)_{12}$-luciferase reporter and cultured under a protocol that resembled the mineralization assay (Figure 2(B)); i.e. 100 ng/ml of either rhBMP-2 or rhBMP-4 were administered on day 5, two days after the commencement of DEX treatment. Based on preliminary experiments, BMP-4 was administered at 100 ng/ml. rhBMP-2 was administered at increasing concentrations (1–100 ng/ml) to assure that the comparison was made under conditions, where Smad activation was not saturated. As shown in Figure 3(A), rhBMP-4 stimulation of BMP–Smad activity was weaker than that of rhBMP-2. In two independent experiments, in which rhBMP treatment lasted either 12 or 24 h, the effect of the 100 ng/ml rhBMP-4 dose was equivalent to an interpolated rhBMP-2 dose of 18–20 ng/ml (Figure 3(A)). Thus, unlike ALP, which was equally activated by the two rhBMPs in DEX-treated MC3T3-E1 cultures (Figure 2(A)), BMP–Smad activity was stimulated 5-fold more strongly by rhBMP-2 as compared to rhBMP-4. Thus, the weaker Smad activation potential of rhBMP-4 (Figure 3(A)) may explain its failure to rescue mineralization in DEX-treated MC3T3-E1 cultures (Figure 2(B)).

The inability of rhBMP-4 to rescue mineralization (Figure 2(B)) could reflect a qualitative inferiority relative to rhBMP-2. However, since the two rhBMPs were only quantitatively different with regard to their Smad activation potential (Figure 3(A)), we suspected that rhBMP-4 would be able to induce mineralization in DEX-treated MC3T3-E1 cultures when either the rhBMP-4 dose was increased to match the BMP–Smad activation potential of rhBMP-2 or the treatment period was extended. We chose the latter, and treated DEX-inhibited cultures for 24 h with either 100 ng/ml of rhBMP-4 or increasing concentrations of rhBMP-2 ranging from 5 to 100 ng/ml. Mineral deposition was assessed on days 12, 13, 14, and 15 by Alizarin Red staining. In contrast to rhBMP-4's failure to restore DEX-inhibited mineralization following 10-h exposure (Figure 2(B)) or 24-h exposure when followed by only 6 or 7-day rescue time (Figure 3, days 12 and 13), the 24-h rhBMP-4 pulse induced mineralization in DEX-cultures after 8 days (Figure 3(B), day 14) and more, so after 9 days (day 15). As expected, however, the rhBMP-2-mediated rescue was more robust, with marked calcium deposition observed already on day 12, after exposure to not only the 100 ng/ml dose, but also the 50 ng/ml dose (Figure 3(B)). By day 14, the cultures which had been exposed to 20 ng/ml rhBMP-2 resembled those that had been exposed to 100 ng/ml rhBMP-4. Thus, both rhBMP-2 and rhBMP-4 induced calcium deposition in DEX-inhibited MC3T3-E1 cultures, with rhBMP-2 displaying approximately 5-fold greater potency. Taken together, Figures 2 and 3 demonstrate that Smad activity, not ALP activity, could predict the relative rhBMP doses required to rescue mineral deposition.

DEX does not strongly inhibit transcription from the 2.7 kb proximal *Bmp2* promoter

Based on the low basal expression of *Bmp2* and the persistence of normal BMP–Smad activity in DEX-treated cultures (Figure 1), it appears that inhibition of *Bmp2* gene expression is a marker for, rather than the cause of the phenotype suppression in GC-treated MC3T3-E1 cultures. However, since the regulation of *BMP2* gene expression is likely critical for bone mass control *in vivo* (Styrkarsdottir et al. 2003), we initiated a study to map GC-responsive element(s) at the *Bmp2* locus.

Published studies have demonstrated that estrogen (Zhou et al. 2003), retinoic acid (Heller et al. 1999), and statins (Mundy et al. 1999) regulate *Bmp2* transcription through a 2.7 kb region upstream of the *Bmp2* transcription start site. We tested the effect of DEX on this region with a luciferase reporter driven by a 2712 bp fragment of the *Bmp2* promoter. As seen in Figure 4, DEX did not significantly inhibit transcription of the −2712 bp *Bmp2* promoter–reporter at 4, 24, or 48 h; the latter corresponded to the time point when *Bmp2* mRNA was markedly suppressed (Figure 1(B)). DEX treatment also did not alter

transactivation of luciferase reporters encompassing 5′ deletion mutants (1997 and 838 bp) of the *Bmp2* proximal promoter (data not shown).

DEX counteracts activity of a far-downstream *Bmp2* transcriptional regulatory domain

Even though the *Bmp2* proximal promoter contains several hormone-responsive elements (Heller et al. 1999; Mundy et al. 1999; Zhou et al. 2003) we were not surprised that it did not respond to DEX (Figure 4) because TGF-β family genes (DiLeone et al. 1998; Mortlock et al. 2003), including *Bmp2* (Chandler et al. 2007), are also regulated through distal elements. To address the contribution of distal cis-regulatory elements to DEX-mediated *Bmp2* gene repression, we used two overlapping BAC reporter constructs, which together spanned 392 kb of the mouse *Bmp2* locus. The 3′ BAC construct contained sequences between positions −2.7 and +207.1 kb, and the 5′ BAC contained sequences between −185.4 and +53.7 kb. In both BACs, exon 3 of the *Bmp2* gene was engineered to contain the LacZ/Neo fusion reporter (Figure 5(A)). MC3T3-E1 osteoblasts were transfected with either the 3′ or 5′ *Bmp2*-LacZ BAC constructs, and stable cell pools carrying each BAC were generated by neomycin selection. The effects of DEX on *Bmp2*-LacZ transgene expression were determined by X-gal staining and biochemical measurement of β-galactosidase activity at several time points during the development of the osteoblast phenotype. Similar to our observations *in vivo* (Chandler et al. 2007), only expression of the 3′ BAC was readily detectable in the MC3T3-E1 cultures (Figure 5(B)). Blue X-gal staining was first observed on day 6, and then intensified throughout the experiment. By contrast, no X-gal staining was seen at any time point in cell cultures containing the 5′ BAC (Figure 5(B); day 11 is shown). DEX treatment strongly inhibited X-gal staining in the 3′ BAC lines at all time points (Figure 5).

Microscopic observation of the X-gal-stained cultures on day 6 and 11, highlighted the differences in culture morphology and 3′ BAC expression between CONTROL and DEX cultures (Figure 5(C)). In day 6 CONTROL cultures, X-gal staining was randomly distributed among individual cells. By day 11, the blue staining was mostly observed in areas of condensation where nodule formation had begun. By contrast, few cells in the DEX-treated cultures stained blue, and the cultures failed to condense.

The biochemical measurement of β-gal activity on day 11 (Figure 5(D)) supported the staining results. β-gal activity was robust in the 3′ BAC-containing CONTROL cultures and was strongly inhibited by DEX. Although, it was difficult to observe by histological staining, β-gal activity above background levels (i.e. untransfected MC3T3-E1 cultures) was measured in the 5′ BAC cultures, but was only slightly inhibited by DEX. These findings are consistent with our *in vivo* results that identified an osteoblast-specific cis-acting regulatory element far downstream of the *Bmp2* gene, between positions +53 and +207 kb (Chandler et al. 2007). Furthermore, the present study indicates that the same or other elements within the +53/+207-kb domain are responsible for the DEX-mediated *Bmp2* gene repression.

Discussion

Inhibition of *Bmp2* expression is not critical for the phenotype suppression in GC-treated MC3T3-E1 cells

While, GCs adversely affect osteoblast function and bone formation *in vivo*, both positive and negative GC effects have been reported in a variety of culture systems; and GCs have been shown to cooperate with BMPs in some culture systems (Cooper et al. 1999). Deleterious effects of GCs on osteoblasts *in vitro* are most readily demonstrable in murine culture models. We have previously shown that DEX inhibits *Bmp2* gene expression

(Luppen et al. 2003a) and mineralization in MC3T3-E1 osteoblast cultures (Lian et al. 1997; Luppen et al. 2003b; Smith et al. 1999), and that rhBMP-2 rescues mineralization in this model system (Luppen et al. 2003a,b). It was tempting to conclude that treatment with the recombinant protein simply reversed the loss of the endogenous *Bmp2* gene product. Although, such interpretation has not been ruled out, the results of the present study suggest otherwise. We propose that GC inhibition of *Bmp2* is secondary to the inhibition of the osteoblast phenotype. Indeed, we showed that GCs suppressed mineralization in MC3T3-E1 cultures without significantly inhibiting two BMP effectors: ALP (Luppen et al. 2003a) and BMP–Smad activity (Figure 1(D)). Therefore, we believe that rhBMP-2 (Luppen et al. 2003a,b) and rhBMP-4 (Figure 3) did not rescue mineral deposition by simply reversing the GC inhibition of *Bmp2*.

How did BMP–Smad (Figure 1(D)) and ALP (Luppen et al. 2003a) activities persist in the face of the strong *Bmp2* suppression in GC-treated MC3T3-E1 cultures? Likely, other endogenous BMPs with osteogenic activities (e.g. BMP-4, 5–7, and 9) overshadowed the GC-suppression of *Bmp2* in this system. For example, *Bmp4* mRNA levels, which far exceeded basal *Bmp2* mRNA levels (Figure 1(C)), were not affected by GCs. The expression of other osteogenic BMPs, however, would not necessarily rule out a functional significance for the *Bmp2* suppression. In order to ascribe biological relevance to the GC-suppression of *Bmp2* mRNA, one could hypothesize, for example, far more efficient post-RNA processing of BMP-2. In support of this, the lowest rhBMP-2 dose that induced some mineralization in DEX-treated cultures (5 ng/ml, Figure 3(B)) produced in the luciferase assays (Figure 3(A)) a signal in the same order of magnitude as that measured in untreated cultures (Figure 1(D)). An alternate hypothesis is that there may be a unique function for BMP-2 in osteoblasts that BMP-4 is unable to fulfill. Such a difference between BMP-2 and BMP-4 would be consistent with the impaired bone mass acquisition and development of spontaneous fractures in mouse limbs deficient in *Bmp2* (Tsuji et al. 2006). The requirement for *Bmp2*, however, does not necessarily reflect a unique feature of the protein-coding sequences. It could also reflect *Bmp2* regulatory element(s) responsible for generating a BMP signal under physiological conditions in which other *Bmps*, such as *Bmp4* are differentially regulated. Thus, the GC-mediated suppression might be critical under conditions that require uninterrupted *Bmp2* expression for proper tissue function (as discussed in the following paragraph). In our specific MC3T3-E1 system, however, we believe that this inhibition is a consequence of, not a mechanism by which GCs inhibit mineralization, because GCs did not inhibit the SMAD reporter.

Importance of *Bmp2* transcriptional regulation and mechanism of the GC-mediated inhibition

The GC-suppression of *Bmp2* might become functionally critical in a culture system, in which *Bmp2* was expressed at higher levels than other *Bmp* genes. Although, we are unaware of such an *in vitro* system, the requirement for appropriate BMP2 expression in bone mass control is evidenced by the osteoporosis associated with genetic variants in the human *BMP2* locus (Styrkarsdottir et al. 2003) and by the irreparable fractures that develop in postnatal *Bmp2*-deficient limbs (Tsuji et al. 2006). Thus, the GC-inhibition of *Bmp2* is still important for two reasons. First, GC-inhibition may contribute to GIO in cell types, and under developmental conditions, where BMP-2 contributes significantly to overall BMP signaling. Indeed, despite the strong homology between *Bmp2* and *Bmp4* in their respective coding regions (Celeste et al. 1990), the regulation and regulatory sequences of the two genes are quite diverse (Fritz et al. 2004). Second, *Bmp2* mRNA, not *Bmp4* mRNA, mirrored the osteoblast phenotype at least in the MC3T3-E1 system. *Bmp2* was suppressed along with the loss of mineralization (Figure 1) and rescued along with the rhBMP-2-rescue of mineralization (Luppen et al. 2003b). Thus, mechanisms regulating *Bmp2* expression

may provide novel insights into osteoblast function. For these reasons we decided to exploit the MC3T3-E1 system and map GC negative response elements at the *Bmp2* locus.

Initial transient transfection assays indicated that the 2.7 kb sequence upstream of the *Bmp2* transcription start site was not responsible for the GC-mediated repression (Figure 4). The very weak (if any) GC-responsiveness of a reporter BAC that contained additional 5′ flanking sequences suggested that that the GC-responsive domain was not present upstream of the transcription start site up to position −185 kb (Figure 5). The results with this 5′ BAC also suggest that the GC-responsive domain is not located within either BMP-2 coding sequences or 3′ flanking sequences down to position +53 kb (Figure 5). Remarkably, however, a reporter BAC that extended downstream to position +207 kb was strongly transcribed, was expressed when and where osteoblastic nodules formed, and was repressed by DEX (Figure 5). Interestingly, distant 3′ sequences are also required for *in vivo* expression of *Bmp2* in osteoblasts (Chandler et al. 2007). The overlap between the GC-responsive sequences and those that mediate basal expression remains to be determined.

Differential effects of rhBMP-2 and rhBMP-4 on ALP, BMP–Smads and mineralization

Recombinant preparations and viral BMP vectors are often compared based on their osteogenic or other biological effects (Boden et al. 1996; Kang et al. 2004; Zhao et al. 2005). Such comparisons must be conducted with caution because viral vectors may not necessarily produce similar amounts of the respective BMPs, and recombinant preparations may vary in protein quality and post-translational modifications. In this regard, it is useful to have accurate bioassays that measure BMP activities. In the present study, we employed two such assays. One was activation of ALP using the *p*-nitrophenol colorimetric assay. For the second assay, we used a specific BMP-responsive plasmid ($(GCCG)_{12}$-luciferase) and generated a stable cell line that reports on BMP–Smad activity. Remarkably, the two assays provided different results. While comparable doses of the rhBMP-2 and rhBMP-4 preparations used in this study equally stimulated ALP, 5-fold higher doses of the rhBMP-4 preparation were needed for equivalent activation of BMP–Smads. Similar to Smad activation, the rhBMP-2 preparation was approximately 5-fold more potent than the rhBMP-4 preparation in inducing mineralization in our system. Is BMP-2 generally more osteogenic than BMP-4? Is BMP-2 more osteogenic specifically in GC-arrested MC3T3-E1 cultures?

Before discussing possible differences between BMP-2 and BMP-4, it is worth noting the synergy between GC and BMP-2 signaling. As seen in Figure 1(D), rhBMP-2 induction of Smad signaling was significantly augmented in DEX-treated compared to CONTROL cultures. This synergy is consistent with previous findings from our and other labs (Centrella et al. 1997; Luppen et al. 2003a). We speculate that DEX treatment may return the relatively differentiated MC3T3-E1 osteoblasts to a more naïve state, in which the cultures are more responsive to exogenous BMP-2.

BMP-2 and BMP-4 are highly homologous (Celeste et al. 1990), they interact with BMP receptors with comparable affinities (Kirsch et al. 2000; Sebald et al. 2004) and are equally osteogenic in other systems (Cheng et al. 2003). We propose that an explanation for the observed differences between BMP-2 and BMP-4 in our system may be that GC-treated MC3T3-E1 cells could express a protein that either confers preferential Smad activation specifically on BMP-2, or specifically inhibits BMP-4 induced Smad activation. Such a protein could be, for example, a membrane-associated or secreted molecule that simultaneously interacts with: (i) BMP receptor found in a conformation that preferentially stimulates Smad-dependent signaling (Nohe et al. 2002), and (ii) the N-terminus of the mature BMP-2, which, unlike the rest of the protein, is different from the respective domain of BMP-4 (Ohkawara et al. 2002). In the present study, the differential outcome of treatment

with rhBMP-2 vs. rhBMP-4, regardless of whether it reflected a difference between the two primary sequences or between the respective manufacturing processes (see Materials and methods), allowed us to obtain strong evidence that activation of BMP–Smads, not ALP, is more relevant to the rescue of mineralization in GC-treated MC3T3-E1 cultures. Further supporting a more important role for Smad signaling in BMP-2-mediated rescue of mineralization in GC-treated MC3T3 system, down-regulation of ALP activity with MAP Kinase inhibitors did not interfere with BMP-induced mineralization (data not shown). Intriguingly, Nohe et al. (2002) have shown that two BMPR configurations, one ligand-induced and the other preformed, code for MAP Kinase and SMAD signaling, respectively.

In conclusion, by comparing the activities of two rhBMP preparations in GC-treated osteoblast cultures, we were able to demonstrate that mineralization could not be predicted based on stimulation of ALP. The two preparations, one of rhBMP-2 and one of rhBMP-4, equally rescued mineralization, when administered such that the BMP–Smads were equally stimulated. Whereas, the molecular basis for the differential ALP vs. SMAD activation may be difficult to decipher, our work sheds light on the respective contributions of Smad-dependent vs. Smad-independent BMP signaling to bone-like tissue formation in MC3T3-E1 osteoblast cultures.

Acknowledgments

The authors thank Drs Ming Zhao and Stephen Harris (University of Texas Health Sciences Center, San Antonio, TX) for *Bmp2* promoter-luciferase constructs and the BMP–Smad reporter "$(GCCG)_{12}$-luciferase"; Wyeth Pharmaceuticals (Cambridge, MA) for rhBMP-2; and Drs Johnny Huard (University of Pittsburgh) and Wei Zhu (Hospital for Special Surgery, New York, NY, USA) for helpful discussions. This study was supported by grants from the Arthritis Foundation (Atlanta, Georgia, to BF) and the NIH (AR047052 to BF and HD47880-01 to DPM) and by the J. Harold and Edna L. LaBriola Chair in Genetic Orthopaedics at the University of Southern California (held by BF). CAL and RLC were supported by NIH training grants DE07211 and HD07502, respectively. The experiments were conducted in a facility constructed with support from Research Facilities Improvement Program Grant Number C06 (RR10600-01, CA62528-01, RR14514-01) from the NIH/NCRR.

References

Abzhanov A, Protas M, Grant BR, Grant PR, Tabin CJ. Bmp4 and morphological variation of beaks in Darwin's finches. Science. 2004; 305(5689):1462–1465. [PubMed: 15353802]

Boden SD, McCuaig K, Hair G, Racine M, Titus L, Wozney JM, Nanes MS. Differential effects and glucocorticoid potentiation of bone morphogenetic protein action during rat osteoblast differentiation *in vitro*. Endocrinology. 1996; 137(8):3401–3407. [PubMed: 8754767]

Canalis E, Delany AM. Mechanisms of glucocorticoid action in bone. Ann N Y Acad Sci. 2002; 966:73–81. [PubMed: 12114261]

Celeste AJ, Iannazzi JA, Taylor RC, Hewick RM, Rosen V, Wang EA, Wozney JM. Identification of transforming growth factor beta family members present in bone-inductive protein purified from bovine bone. Proc Natl Acad Sci USA. 1990; 87(24):9843–9847. [PubMed: 2263636]

Centrella M, Rosen V, Wozney JM, Casinghino SR, McCarthy TL. Opposing effects by glucocorticoid and bone morphogenetic protein-2 in fetal rat bone cell cultures. J Cell Biochem. 1997; 67(4):528–540. [PubMed: 9383711]

Chandler RL, Chandler KJ, McFarland KA, Mortlock DP. Bmp2 transcription in osteoblast progenitors is regulated by a distant 3′ enhancer located 156.3 kilobases from the promoter. Mol Cell Biol. 2007; 27:2934–2951. [PubMed: 17283059]

Cheng H, Jiang W, Phillips FM, Haydon RC, Peng Y, Zhou L, Luu HH, An N, Breyer B, Vanichakarn P, et al. Osteogenic activity of the fourteen types of human bone morphogenetic proteins (BMPs). J Bone Joint Surg Am. 2003; 85-A(8):1544–1552. [PubMed: 12925636]

Cooper MS, Hewison M, Stewart PM. Glucocorticoid activity, inactivity and the osteoblast. J Endocrinol. 1999; 163(2):159–164. [PubMed: 10556763]

Dempster DW, Moonga BS, Stein LS, Horbert WR, Antakly T. Glucocorticoids inhibit bone resorption by isolated rat osteoclasts by enhancing apoptosis. J Endocrinol. 1997; 154(3):397–406. [PubMed: 9379116]

Derynck R, Zhang YE. Smad-dependent and Smad-independent pathways in TGF-beta family signalling. Nature. 2003; 425(6958):577–584. [PubMed: 14534577]

DiLeone RJ, Russell LB, Kingsley DM. An extensive 3′ regulatory region controls expression of Bmp5 in specific anatomical structures of the mouse embryo. Genetics. 1998; 148(1):401–408. [PubMed: 9475750]

Feng XH, Derynck R. Specificity and versatility in tgf-beta signaling through Smads. Annu Rev Cell Dev Biol. 2005; 21:659–693. [PubMed: 16212511]

Fritz DT, Liu D, Xu J, Jiang S, Rogers MB. Conservation of Bmp2 post-transcriptional regulatory mechanisms. J Biol Chem. 2004; 279(47):48950–48958. [PubMed: 15358784]

Godschalk MF, Downs RW. Effect of short-term glucocorticoids on serum osteocalcin in healthy young men. J Bone Miner Res. 1988; 3(1):113–115. [PubMed: 3264991]

Greenwald J, Vega ME, Allendorph GP, Fischer WH, Vale W, Choe S. A flexible activin explains the membrane-dependent cooperative assembly of TGF-beta family receptors. Mol Cell. 2004; 15(3): 485–489. [PubMed: 15304227]

Guicheux J, Lemonnier J, Ghayor C, Suzuki A, Palmer G, Caverzasio J. Activation of p38 mitogen-activated protein kinase and c-Jun-NH2-terminal kinase by BMP-2 and their implication in the stimulation of osteoblastic cell differentiation. J Bone Miner Res. 2003; 18(11):2060–2068. [PubMed: 14606520]

Harrison CA, Gray PC, Fischer WH, Donaldson C, Choe S, Vale W. An activin mutant with disrupted ALK4 binding blocks signaling via type II receptors. J Biol Chem. 2004; 279(27):28036–28044. [PubMed: 15123686]

Heller LC, Li Y, Abrams KL, Rogers MB. Transcriptional regulation of the Bmp2 gene. Retinoic acid induction in F9 embryonal carcinoma cells and Saccharomyces cerevisiae. J Biol Chem. 1999; 274(3):1394–1400. [PubMed: 9880512]

Hu Y, Chan E, Wang SX, Li B. Activation of p38 mitogen-activated protein kinase is required for osteoblast differentiation. Endocrinology. 2003; 144(5):2068–2074. [PubMed: 12697715]

Kang Q, Sun MH, Cheng H, Peng Y, Montag AG, Deyrup AT, Jiang W, Luu HH, Luo J, Szatkowski JP, et al. Characterization of the distinct orthotopic bone-forming activity of 14 BMPs using recombinant adenovirus-mediated gene delivery. Gene Ther. 2004; 11(17):1312–1320. [PubMed: 15269709]

Kent WJ, Sugnet CW, Furey TS, Roskin KM, Pringle TH, Zahler AM, Haussler D. The human genome browser at UCSC. Genome Res. 2002; 12(6):996–1006. [PubMed: 12045153]

Kirsch T, Sebald W, Dreyer MK. Crystal structure of the BMP-2-BRIA ectodomain complex. Nat Struct Biol. 2000; 7(6):492–496. [PubMed: 10881198]

Kusanagi K, Inoue H, Ishidou Y, Mishima HK, Kawabata M, Miyazono K. Characterization of a bone morphogenetic protein-responsive Smad-binding element. Mol Biol Cell. 2000; 11(2):555–565. [PubMed: 10679014]

Lai CF, Cheng SL. Signal transductions induced by bone morphogenetic protein-2 and transforming growth factor-beta in normal human osteoblastic cells. J Biol Chem. 2002; 277(18):15514–15522. [PubMed: 11854297]

Leclerc N, Luppen CA, Ho VV, Nagpal S, Hacia JG, Smith E, Frenkel B. Gene expression profiling of glucocorticoid-inhibited osteoblasts. J Mol Endocrinol. 2004; 33(1):175–193. [PubMed: 15291752]

Lian JB, Shalhoub V, Aslam F, Frenkel B, Green J, Hamrah M, Stein GS, Stein JL. Species-specific glucocorticoid and 1,25-dihydroxyvitamin D responsiveness in mouse MC3T3-E1 osteoblasts: Dexamethasone inhibits osteoblast differentiation and vitamin D down-regulates osteocalcin gene expression. Endocrinology. 1997; 138(5):2117–2127. [PubMed: 9112412]

Liu W, Selever J, Murali D, Sun X, Brugger SM, Ma L, Schwartz RJ, Maxson R, Furuta Y, Martin JF. Threshold-specific requirements for Bmp4 in mandibular development. Dev Biol. 2005; 283(2): 282–293. [PubMed: 15936012]

Liu Y, Titus L, Barghouthi M, Viggeswarapu M, Hair G, Boden SD. Glucocorticoid regulation of human BMP-6 transcription. Bone. 2004; 35(3):673–681. [PubMed: 15336603]

Luppen CA, Leclerc N, Noh T, Barski A, Khokhar A, Boskey AL, Smith E, Frenkel B. Brief bone morphogenetic protein 2 treatment of glucocorticoid-inhibited MC3T3-E1 osteoblasts rescues commitment-associated cell cycle and mineralization without alteration of Runx2. J Biol Chem. 2003a; 278(45):44995–45003. [PubMed: 12933820]

Luppen CA, Smith E, Spevak L, Boskey AL, Frenkel B. Bone morphogenetic protein-2 restores mineralization in glucocorticoid-inhibited MC3T3-E1 osteoblast cultures. J Bone Miner Res. 2003b; 18(7):1186–1197. [PubMed: 12854828]

Mazziotti G, Angeli A, Bilezikian JP, Canalis E, Giustina A. Glucocorticoid-induced osteoporosis: An update. Trends Endocrinol Metab. 2006; 17(4):144–149. [PubMed: 16678739]

Melkonyan H, Sorg C, Klempt M. Electroporation efficiency in mammalian cells is increased by dimethyl sulfoxide (DMSO). Nucleic Acids Res. 1996; 24(21):4356–4357. [PubMed: 8932394]

Mortlock DP, Guenther C, Kingsley DM. A general approach for identifying distant regulatory elements applied to the Gdf6 gene. Genome Res. 2003; 13(9):2069–2081. [PubMed: 12915490]

Mundy G, Garrett R, Harris S, Chan J, Chen D, Rossini G, Boyce B, Zhao M, Gutierrez G. Stimulation of bone formation *in vitro* and in rodents by statins. Science. 1999; 286(5446):1946–1949. [PubMed: 10583956]

Nohe A, Hassel S, Ehrlich M, Neubauer F, Sebald W, Henis YI, Knaus P. The mode of bone morphogenetic protein (BMP) receptor oligomerization determines different BMP-2 signaling pathways. J Biol Chem. 2002; 277(7):5330–5338. [PubMed: 11714695]

O'Brien CA, Jia D, Plotkin LI, Bellido T, Powers CC, Stewart SA, Manolagas SC, Weinstein RS. Glucocorticoids act directly on osteoblasts and osteocytes to induce their apoptosis and reduce bone formation and strength. Endocrinology. 2004; 145(4):1835–1841. [PubMed: 14691012]

Ohkawara B, Iemura S, ten Dijke P, Ueno N. Action range of BMP is defined by its N-terminal basic amino acid core. Curr Biol. 2002; 12(3):205–209. [PubMed: 11839272]

Owen TA, Aronow M, Shalhoub V, Barone LM, Wilming L, Tassinari MS, Kennedy MB, Pockwinse S, Lian JB, Stein GS. Progressive development of the rat osteoblast phenotype *in vitro*: Reciprocal relationships in expression of genes associated with osteoblast proliferation and differentiation during formation of the bone extracellular matrix. J Cell Physiol. 1990; 143(3):420–430. [PubMed: 1694181]

Pearce G, Tabensky DA, Delmas PD, Baker HW, Seeman E. Corticosteroid-induced bone loss in men. J Clin Endocrinol Metab. 1998; 83(3):801–806. [PubMed: 9506731]

Peng H, Usas A, Olshanski A, Ho AM, Gearhart B, Cooper GM, Huard J. VEGF improves, whereas sFlt1 inhibits, BMP2-induced bone formation and bone healing through modulation of angiogenesis. J Bone Miner Res. 2005; 20(11):2017–2027. [PubMed: 16234975]

Prummel MF, Wiersinga WM, Lips P, Sanders GT, Sauerwein HP. The course of biochemical parameters of bone turnover during treatment with corticosteroids. J Clin Endocrinol Metab. 1991; 72(2):382–386. [PubMed: 1991808]

Qiao B, Padilla SR, Benya PD. Transforming growth factor (TGF)-beta-activated kinase 1 mimics and mediates TGF-beta-induced stimulation of type II collagen synthesis in chondrocytes independent of Col2a1 transcription and Smad3 signaling. J Biol Chem. 2005; 280(17):17562–17571. [PubMed: 15743758]

Sears KE, Behringer RR, Rasweiler JJt, Niswander LA. Development of bat flight: Morphologic and molecular evolution of bat wing digits. Proc Natl Acad Sci USA. 2006; 103(17):6581–6586. [PubMed: 16618938]

Sebald W, Nickel J, Zhang JL, Mueller TD. Molecular recognition in bone morphogenetic protein (BMP)/receptor interaction. Biol Chem. 2004; 385(8):697–710. [PubMed: 15449706]

Smith E, Redman RA, Logg CR, Coetzee GA, Kasahara N, Frenkel B. Glucocorticoids inhibit developmental stage-specific osteoblast cell cycle. Dissociation of cyclin A-cdk2 from E2F4-p130 complexes. J Biol Chem. 1999; 275(26):2–20001.

Styrkarsdottir U, Cazier JB, Kong A, Rolfsson O, Larsen H, Bjarnadottir E, Johannsdottir VD, Sigurdardottir MS, Bagger Y, Christiansen C, et al. Linkage of Osteoporosis to Chromosome 20p12 and Association to BMP2. PLoS Biol. 2003; 1(3):E69. [PubMed: 14691541]

Sudo H, Kodama HA, Amagai Y, Yamamoto S, Kasai S. *In vitro* differentiation and calcification in a new clonal osteogenic cell line derived from newborn mouse calvaria. J Cell Biol. 1983; 96(1): 191–198. [PubMed: 6826647]

Tsuji K, Bandyopadhyay A, Harfe BD, Cox K, Kakar S, Gerstenfeld L, Einhorn T, Tabin CJ, Rosen V. BMP2 activity, although dispensable for bone formation, is required for the initiation of fracture healing. Nat Genet. 2006; 38(12):1424–1429. [PubMed: 17099713]

Urist MR. Bone: Formation by autoinduction. Science. 1965; 150(698):893–899. [PubMed: 5319761]

Van Staa TP, Leufkens HG, Abenhaim L, Zhang B, Cooper C. Use of oral corticosteroids and risk of fractures. J Bone Miner Res. 2000; 15(6):993–1000. [PubMed: 10841167]

Wang D, Christensen K, Chawla K, Xiao G, Krebsbach PH, Franceschi RT. Isolation and characterization of MC3T3-E1 preosteoblast subclones with distinct *in vitro* and *in vivo* differentiation/mineralization potential. J Bone Miner Res. 1999; 14(6):893–903. [PubMed: 10352097]

Weinstein RS, Jilka RL, Parfitt AM, Manolagas SC. Inhibition of osteoblastogenesis and promotion of apoptosis of osteoblasts and osteocytes by glucocorticoids. Potential mechanisms of their deleterious effects on bone. J Clin Invest. 1998; 102(2):274–282. [PubMed: 9664068]

Wu P, Jiang TX, Suksaweang S, Widelitz RB, Chuong CM. Molecular shaping of the beak. Science. 2004; 305(5689):1465–1466. [PubMed: 15353803]

Yu L, Hebert MC, Zhang YE. TGF-beta receptor-activated p38 MAP kinase mediates Smad-independent TGF-beta responses. Embo J. 2002; 21(14):3749–3759. [PubMed: 12110587]

Zalavras C, Shah S, Birnbaum MJ, Frenkel B. Role of apoptosis in glucocorticoid-induced osteoporosis and osteonecrosis. Crit Rev Eukaryot Gene Expr. 2003; 13(2–4):221–235. [PubMed: 14696969]

Zhao M, Harris SE, Horn D, Geng Z, Nishimura R, Mundy GR, Chen D. Bone morphogenetic protein receptor signaling is necessary for normal murine postnatal bone formation. J Cell Biol. 2002; 157(6):1049–1060. [PubMed: 12058020]

Zhao M, Zhao Z, Koh JT, Jin T, Franceschi RT. Combinatorial gene therapy for bone regeneration: Cooperative interactions between adenovirus vectors expressing bone morphogenetic proteins 2, 4, and 7. J Cell Biochem. 2005; 95(1):1–16. [PubMed: 15759283]

Zhou S, Turgeman G, Harris SE, Leitman DC, Komm BS, Bodine PV, Gazit D. Estrogens activate bone morphogenetic protein-2 gene transcription in mouse mesenchymal stem cells. Mol Endocrinol. 2003; 17(1):56–66. [PubMed: 12511606]

Zhu W, Kim J, Cheng C, Rawlins BA, Boachie-Adjei O, Crystal RG, Hidaka C. Noggin regulation of bone morphogenetic protein (BMP) 2/7 heterodimer activity *in vitro*. Bone. 2006; 39(1):61–71. [PubMed: 16488673]

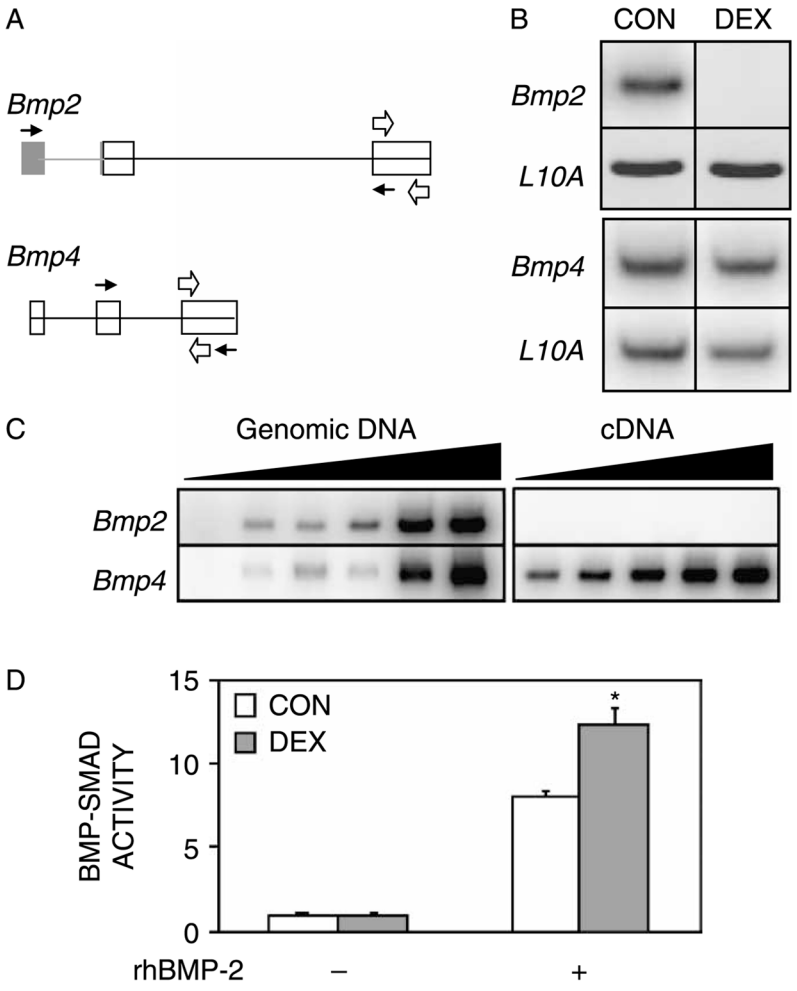

Figure 1.

DEX inhibits *Bmp2* expression, but not *Bmp4* expression or BMP–Smad activity. MC3T3-E1 cultures were analyzed on day 5, 48 h after administration of DEX (1 μM). (A) Schematic of *Bmp2* and *Bmp4* genes. Coding and non-coding exonic sequences are depicted in white and gray, respectively. Black and white arrows represent primers used in Panels B and C, respectively. (B) Representative RT-PCR analysis of *Bmp2*, *Bmp4*, and *L10A mRNA* following DEX treatment. RT-PCR was conducted using intron-spanning primers under. To obtain a clear signal within close-to-linear conditions, the cDNA input used to measure *Bmp2* (*top*) was 21-fold greater than that used to measure *Bmp4* (*bottom*). (C) Comparison between *Bmp2* and *Bmp4* expression in MC3T3-E1 cells. *Left, Bmp2* and *Bmp4* sequences were amplified from genomic DNA using primers that target a single exon in each case. Increasing amounts of genomic DNA were used at 5-fold increments. Note comparable signals for the two genes. *Right*, increasing amounts of cDNA (2-fold increments) were PCR-amplified with the same primers as those used on the left. (D) Effect of DEX on BMP–Smad activity. Cultures stably transfected with the $(GCCG)_{12}$-luciferase reporter were treated for 48 h with 1 μM DEX and/or 100 ng/ml rhBMP-2 as indicated. Luciferase activity is expressed relative to the mean CONTROL value, defined as 1. Mean ± SD; $n = 3$. *$p < 0.05$ compared to CONTROL.

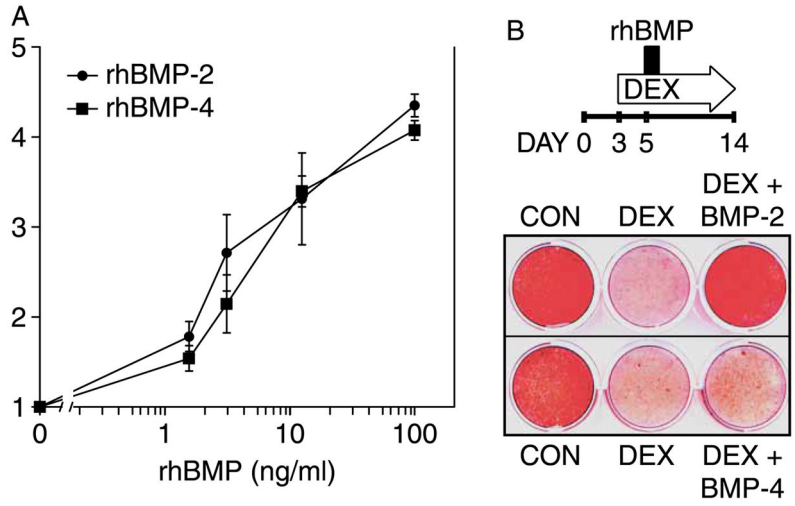

Figure 2.

rhBMP-2 and rhBMP-4 comparably induce ALP activity but not mineralization in DEX-inhibited cultures. MC3T3-E1 cultures were treated with 1 μM DEX commencing on day 3 and with rhBMP-2 or rhBMP-4, 2 days later. (A) ALP activity was measured biochemically 24 h after administration of rhBMP-2 or rhBMP-4 at concentrations between 0.1–100 ng/ml. ALP activity was corrected for DNA content, and the fold stimulation was calculated relative to cultures not treated with BMP. Mean ± SD; $n = 3$. (B) *Top*, schematic illustration of the experimental design. Cultures were treated chronically with 1 μM DEX and exposed to 100 ng/ml rhBMP-2 or -4 for a brief 10-h period on day 5. *Bottom*, Alizarin Red staining of calcium deposition on day 14. Stained plate is representative of three experiments with similar results.

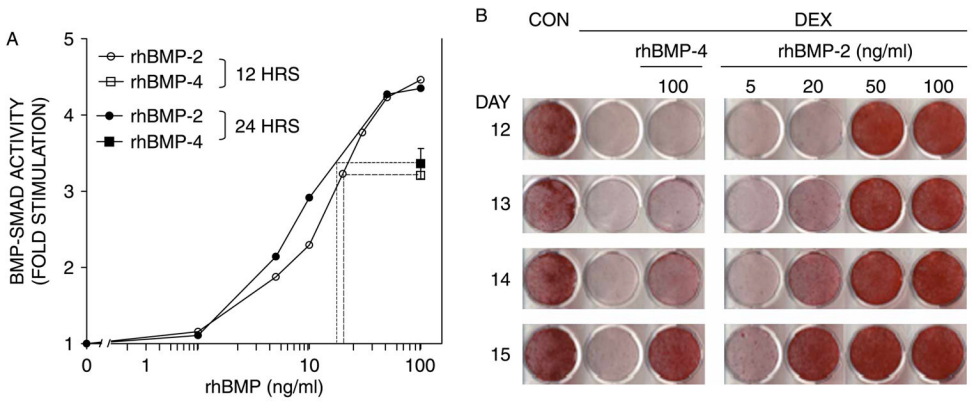

Figure 3.

Differential stimulation of BMP–Smads by rhBMP-2 and -4 parallels mineralization. MC3T3-E1 cultures were treated with 1 μM DEX starting on day 3, followed by a pulse of rhBMP-2 or rhBMP-4 on day 5. (A) Fold stimulation of BMP–Smad activity in two experiments where rhBMP-2 and rhBMP-4 were administered at the indicated concentrations for 12 h (empty) or 24 h (filled symbols). For each of the 12 and 24-h assays, a dashed line projects the activity induced by 100 ng/ml of rhBMP-4 onto the rhBMP-2 curve and graphically determines the rhBMP-2 concentration that is equivalent to 100 ng/ml of rhBMP-4 in this assay. Points with error bars represent mean ± SD ($n = 3$). (B) Cultures were chronically treated with 1 μM DEX starting on day 3 and transiently exposed to rhBMP-2 or -4 at the indicated concentrations for 24 h. Calcium deposition was evaluated between days 12 and 15 by Alizarin Red staining.

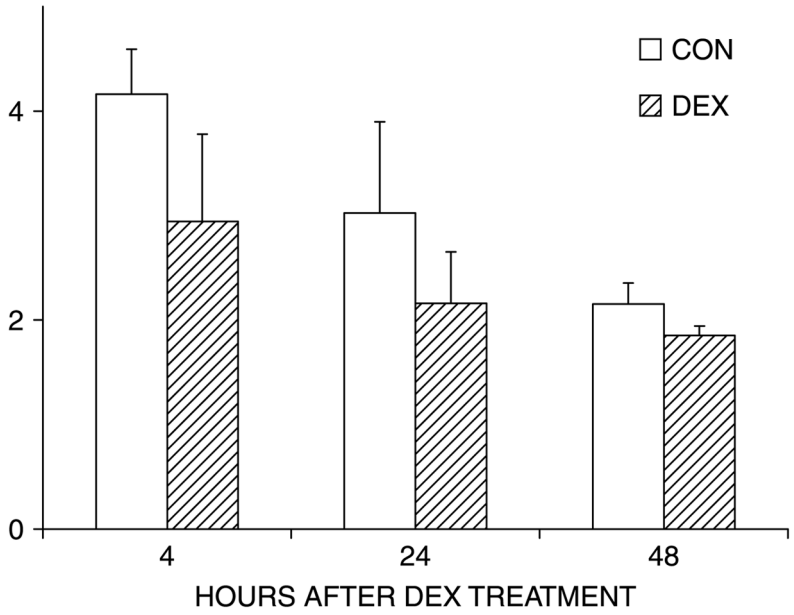

Figure 4.

DEX does not significantly inhibit transcription from the proximal *Bmp2* promoter. MC3T3-E1 cultures were transiently transfected with a reporter construct that contains the 2712 bp *Bmp2* promoter upstream of the firefly luciferase gene. DEX (1 μM) was administered when cultures reached confluency. Cell lysates were analyzed for luciferase activity following 4, 24, and 48 h after DEX treatment. Luciferase activity (relative light units) was corrected for total protein, and the graph shows the mean ± SD of triplicate cultures from a representative experiment.

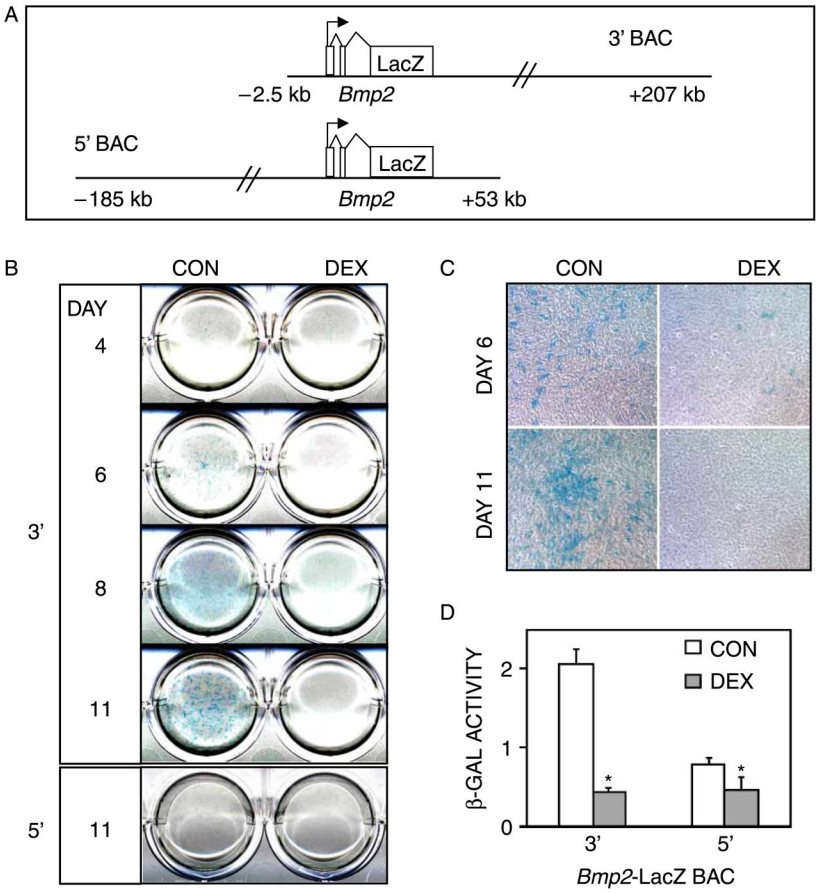

Figure 5.

DEX inhibits *Bmp2* expression via far-downstream regulatory element(s). MC3T3-E1 cultures were stably transfected with *Bmp2*-LacZ BAC reporter constructs, and treated with 1 μM DEX starting on day 3. (A) Schematic illustration of the 3′ and 5′ BAC constructs. (B) X-gal staining of days 4–11 cultures stably transfected with the 3′ BAC. Similar staining was seen in three independent 3′ BAC lines. Two independent lines that were stably transfected with the 5′ BAC construct did not stain for β-gal at any time point; only day 11 is shown for one of the 5′ BAC lines. (C) Micrographs of cultures from *B*, showing X-gal staining of condensing areas in CONTROL cultures, and sparse staining in DEX-treated cultures that failed to condense. Original magnification 100 ×. (D) Biochemical analysis of β-gal activity in day 11-cultures carrying 3′ and 5′ *Bmp2*-BAC constructs. β-gal activity was corrected for total protein. β-gal activity of non-transfected MC3T3-E1 cultures was negligible. Values represent the mean ± SD of triplicate cultures. *$p < 0.05$ compared to CONTROL.

Table I

Primers and conditions used for PCR.

Gene	Accession no.	Primers	Annealing temp.°C	Cycles	Amplicon size (bp)
Bmp2, exon 3	NM_007553	F: 5′-AGT TCT GTC CCC AGT GAC GAG TTT R: 5′-GTA CAA CAT GGA GAT TGC GCT GAG	63	35	708
Bmp4, exon 3	NM_007554	F: 5′-GAG AAC ATC CCA GGG ACC AGT R: 5′-TGT GAT GAG GTG TCC AGG AA	63	35	212
Bmp2	NM_007553	F: 5′-GAC GGA CTG CGG TCT CCT AAA G R: 5′-TCT GCA GAT GTG AGA AAC TCG TCA	64	40	496
Bmp4	NM_007554	F: 5′-GCG CCG TCA TTC CGG ATT AC R: 5′-CAT TGT GAT GGA CTA GTC TG	63	32	402
L10A	U12403	F: 5′-CGC CGC AAG TTT CTG GAG AC R: 5′-CTT GCC AGC CTT GTT TAG GC	61	29	327